2025 6th International Conference on Electronic Communication and Artificial Intelligence (ICECAI)

Two-Step-Search Based Spatio-Temporal Resource Allocation for Task-Oriented Single-Beam Directional Wireless Networks

1st Zheng Wu*
School of Information and Electronics
Beijing Institute of Technology
Beijing, China
* zheng_wu@bit.edu.cn

2nd Yuzhuang Miao
School of Information and Electronics
Beijing Institute of Technology
Beijing, China
3420235061@bit.edu.cn

3rd Dongxuan He
School of Information and Electronics
Beijing Institute of Technology
Beijing, China
dongxuan_he@bit.edu.cn

4th Yuang Cao
School of Information and Electronics
Beijing Institute of Technology
Beijing, China
yuang_cao@bit.edu.cn

5th Hua Wang
School of Information and Electronics
Beijing Institute of Technology
Beijing, China
wanghua@bit.edu.cn

6th Chen Wang
School of Information and Electronics
Beijing Institute of Technology
Beijing, China
chen_wang@bit.edu.cn

2025 6th International Conference on Electronic Communication and Artificial Intelligence (ICECAI) | 979-8-3315-1476-1/25/$31.00 ©2025 IEEE | DOI: 10.1109/ICECAI66283.2025.11170883

***Abstract*—Single-beam directional wireless networks (WNs) offer enhanced throughput and reduced interference through spatially separated beams, but face emerging challenges in task-oriented scenarios, including dynamic value of information (VoI) optimization and task-specific constraints. To handle these challenges effectively, a mathematical model based on integer linear programming (ILP) is established for spatio-temporal resource allocation, with theoretical upper bounds for network capacity and VoI derived through GUROBI optimizer. Subsequently, a heuristic two-step search algorithm (TSA) is proposed to obtain a near-optimal solution, which comprises a modified greedy algorithm (MGA) for feasible scheduling under task and two-hop constraints, followed by a hybrid variable neighborhood search and simulated annealing (VNS-SA) mechanism that combines neighborhood exploration with probabilistic suboptimal solution acceptance. The proposed algorithm is implemented in network simulator 3 (NS-3) to evaluate its performance. The results show that TSA nearly reaches the optimal network capacity and VoI under dynamic interference, outperforming the greedy baseline through its refined global-local search balance. This framework establishes a systematic approach for task-driven resource allocation in single-beam directional WNs by integrating centralized coordination with metaheuristic optimization, which achieves near-optimal adaptability in dynamic environments.**

***Index Terms*—Single-beam directional WNs, task-driven resource allocation, VoI, network capacity.**

I. Introduction

Single-beam directional wireless networks (WNs) have been regarded as a flexible and efficient wireless communication protocol, which have been widely applied in various long-range communication scenarios. Compared to omnidirectional antennas, single-beam directional antennas improve network throughput and reduce interference by focusing the signal transmission direction. However, they also bring new challenges, such as the hidden terminal, the exposed terminal, and the deafness of nodes. These issues get worse in contention-based carrier sense multiple access (CSMA) protocols because it is difficult for the medium access control (MAC) layer scheme to align the antenna with the signal direction [1]. In contrast, time division multiple access (TDMA) protocols avoid conflicts and fully exploit the spatial reuse potential of single-beam directional antennas through network-wide synchronization and slot allocation, providing an effective solution for enhancing the performance of WNs [2]. Meanwhile, task-oriented systems effectively reduce unnecessary resource wastage by matching the information transmitted through links with the tasks at the receiver, which are widely applied in fields such as the Internet of Things (IoT) and edge intelligence (EI) [3] [4]. However, these systems has raised the requirements for task-driven resource allocation based on TDMA in single-beam directional WNs, such as considering task relevance in link scheduling and addressing the value of information (VoI) metric introduced by specific tasks [5].

Due to the requirements of resource allocation in task-oriented scenarios, centralized networks, where a central node is used for unified management, are superior to distributed architectures in terms of task relevance and system performance enhancement. Centralized resource allocation in WNs is typically modeled as a graph coloring problem (GCP), where links assigned the same color are considered conflict-free [6]–[9].

Several traditional optimization algorithms have been proposed to solve GCP. The greedy strategy used in [10] efficiently allocates resource blocks (RBs) to vehicle-to-vehicle links in full-duplex vehicular networks, but its myopic nature often leads to suboptimal outcomes since it only focuses on immediate gains. In contrast, simulated annealing (SA) improves upon this by probabilistically allowing suboptimal moves, helping the algorithm avoid local optima and explore the solution space more globally [11]. However, its performance depends on the cooling schedule, which can lead to premature convergence and prevent the algorithm from reaching global optimum if not properly adjusted. Besides, variable neighborhood search (VNS) addresses these limitations by systematically changing the neighborhood structure during the search, promoting broader exploration and enhancing effectiveness compared to greedy or SA alone [12]. Furthermore, the hybrid variable neighborhood search and simulated annealing (VNS-SA) approach combines the strengths of SA's global exploration and VNS's local refinement to achieve better solution quality [13].

While traditional centralized resource allocation in single-beam directional WNs effectively resolves link interference and optimizes network capacity, the VoI of the data transmitted over links and potential task constraints are not fully considered. In particular, VoI is influenced by dynamic external factors. Fortunately, integer linear programming (ILP), as a mathematical model, is well-suited for analyzing theoretical performance in complex scenarios [14]–[16]. However, the NP-hard nature of ILP makes it intractable for practical deployments due to the high computational complexity. To achieve an effective balance between computational complexity and optimization performance, an efficient task-driven resource allocation algorithm for task-oriented single-beam directional WNs is required.

In this paper, a network model for task-oriented single-beam directional WNs is established. The spatio-temporal resource allocation problem is formulated as an ILP model to address task-specific constraints, and the theoretical upper bound for network capacity and VoI is obtained using the GUROBI optimizer. Subsequently, a heuristic two-step search algorithm, based on modified greedy algorithm and VNS-SA, is designed for practical systems to achieve near-optimal performance. Finally, the performance of the proposed algorithm is validated through network simulator 3 (NS-3).

II. System Model

A. Network Model

Considering a centralized wireless network composed of a central node and a set of edge sub-nodes $\mathcal{N} = \{1, 2, \ldots, n\}$ dispersed in a wide-area two-dimensional space, as illustrated in Fig. 1. The system operates in synchronized slots, where the start of each slot is strictly aligned across all nodes. The central node, equipped with enhanced computational capabilities for resource allocation, assigns detection tasks from the target set $\mathcal{P} = \{1, 2, \ldots, p\}$ to sub-nodes and can establish one-hop connections with other nodes. Each sub-node $i \in \mathcal{N}$ is uniquely mapped to a task $p_i \in \mathcal{P}$, and task assignments are globally broadcasted to ensure mutual awareness among sub-nodes.

Sub-nodes establish connections based on task consistency, i.e., a direct link $l_{ij} \in \mathcal{L} = \{1, 2, \ldots, w\}$ is generated if nodes i and j share the same task ($p_i = p_j$) and are one-hop neighbors which could be validated via pre-recorded neighbor tables. For non-neighboring task-sharing pairs, two-hop communication is enabled through relay nodes selected by an improved AODV protocol [17]. This modified protocol prioritizes relay candidates $k \in \mathcal{N}_i$ (the neighbor set of i) that also satisfy $p_k = p_i$, thereby first-hop link l_{ik} and second-hop link l_{kj} can be generated. To guarantee the effectiveness of two-hop communication, packets must be transmitted through l_{ik} to k before l_{kj} can be scheduled for transmission. Moreover, l_{ik} and l_{kj} must be established in pairs. Each sub-node $i \in \mathcal{N}$ is equipped with a single directional beam antenna, constrained to either transmitting (TX) or receiving (RX) mode per slot. Link activation requires mutual beam alignment, i.e., the TX node's beam must point to the RX node's position, and vice versa.

The network is affected by a rapidly moving jammer m, as depicted in Fig. 1. While link establishment is not disrupted by the interference, the value of packets (VoP) is degraded based on distance, where the packets are generated by the sub-nodes. Conflict relationships between links are captured by the matrix $\mathcal{C} \in \{0, 1\}^{|\mathcal{L}| \times |\mathcal{L}|}$. The elements of this matrix are determined by two types of conflicts. First, an element $\mathcal{C}(l_{ij}, l_{kl})$ is set to 1 if the TX node of link l_{ij} lies within the exclusive region (ER) of another link l_{kl}, as defined in [18], indicating an ER conflict. Second, $\mathcal{C}(l_{ij}, l_{ki})$ is set to 1 if node i acts as the TX in link l_{ij} and as the RX in link l_{ki}, which represents a transceiver mode conflict.

The network's task execution efficiency is quantified by VoI. Sub-nodes generate packets containing target detection data at a frequency determined by the signal round-trip time (RTT). The value of the q-th packet ($\mathcal{V}_{pkt}^q$) is a float within $[\mathcal{V}_{min}, \mathcal{V}_{max}]$, quantified by the signal-to-interference-plus-noise ratio (SINR) of the detection signal. The arithmetic mean $\mathbb{E}[\mathcal{V}_{pkt}^q]$ is affected by the distance d_{mi} between the jammer m and node i, while the variance $\mathrm{Var}(\mathcal{V}_{pkt}^q)$ depends on sub-node mobility and observation angles. Successful task completion requires transmitting N packets, and VoI is defined as the normalized aggregation, given by

$$\mathcal{V}_{info} = \frac{1}{N} \sum_{q=1}^{N} \left(\frac{\mathcal{V}_{pkt}^q - \mathcal{V}_{min}}{\mathcal{V}_{max} - \mathcal{V}_{min}} \right)^{\alpha}, \tag{1}$$

where α is a tuning parameter to amplify ($\alpha > 1$) or compress ($\alpha < 1$) value disparities. For analytical simplicity, VoI is assumed to be the same as both the value of nodes (VoN) and the value of links (VoL).

B. Spatio-Temporal Resource Allocation Problem

The division of time resources follows a hierarchical structure similar to traditional centralized systems, as illustrated in Fig. 2. The temporal structure is organized through sequential fixed-duration frames, where each frame contains a control period followed by a communication period. During the control period, the central node collects task statuses (including VoN) from sub-nodes and executes resource allocation. The subsequent communication period consists of multiple fixed-length resource allocation cycles denoted as $\mathcal{T}$. Each cycle includes k synchronized slots indexed sequentially as $\mathcal{T} = \{1, 2, \ldots, k\}$. For any pair of conflicting links $(l_{ij}, l_{kl}) \in \mathcal{L}$ recorded in the conflict matrix $\mathcal{C}$ (i.e., $\mathcal{C}(l_{ij}, l_{kl}) = 1$), they cannot transmit packets simultaneously. Link $l_{ij} \in \mathcal{L}$ can occupy at most one slot within $\mathcal{T}$ to transmit a single packet, and the set of activated links $\mathcal{A}_c \subseteq \mathcal{L}$ within $\mathcal{T}$ is repeated in each resource allocation cycle. Therefore, it is sufficient to define $\mathcal{A}_c$ within a

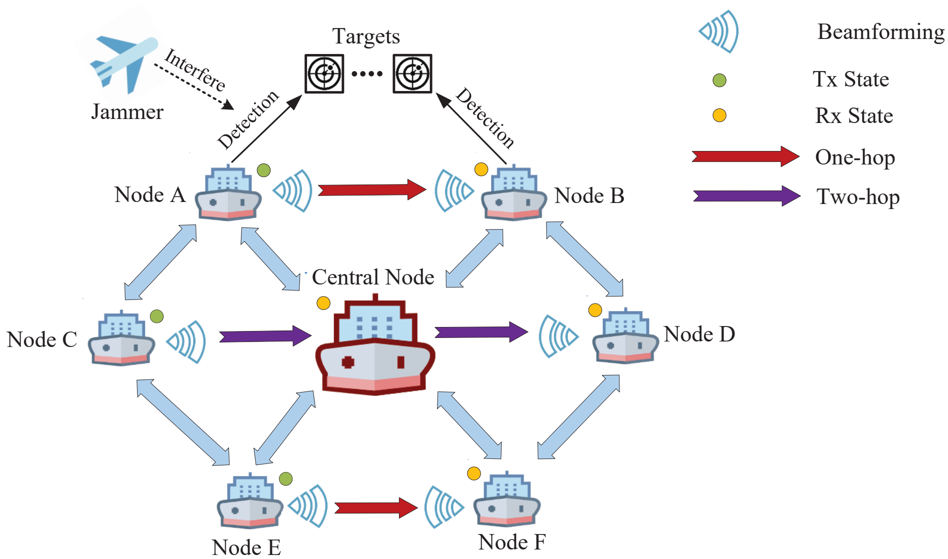

Fig. 1: Centralized wireless network topology diagram.

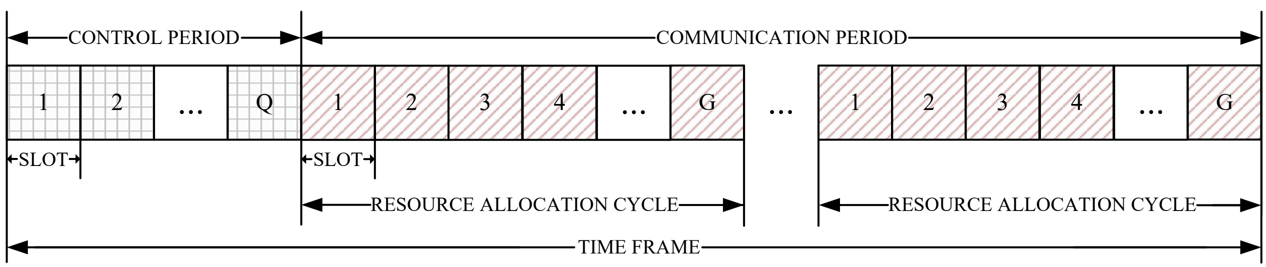

Fig. 2: Time frame structure.

single resource allocation cycle. It is assumed that the number of packets N required to complete the task is equal to the number of $\mathcal{T}$. Once N cycles are executed, the communication period terminates, and the system proceeds to the next frame.

The spatio-temporal resource allocation problem is formally defined as follows. In omnidirectional WNs, successful node communication necessitates complementary transmit-receive states [16]. For networks employing single directional beam antennas, this requirement extends to precise beam alignment between communicating pairs. As depicted in Fig. 1, effective transmission from Node A to Node B requires not only complementary states (A in TX, B in RX) but also mutual beam alignment. This configuration establishes link $l_{AB} \in \mathcal{L}$. Consequently, resource allocation in single-beam directional networks involves specifying nodes' two-dimensional states (transceiver modes and beam directions). Furthermore, our task-oriented architecture simplifies this complexity, i.e., since links are exclusively established between sub-nodes sharing identical tasks ($p_i = p_j$), spatio-temporal resource allocation problem is simplified to link scheduling, i.e., selecting $\mathcal{A}_c$ per frame. In this paper, the task constraint is defined as the requirement that each sub-node $i \in \mathcal{N}$ be connected to at least one source node $j \in \mathcal{N} \setminus \{i\}$ with identical task assignment $p_i = p_j$.

III. Mathematical Modeling and Heuristic Two-Step Search Algorithm Design

A. Mathematical Modeling of Network Capacity and VoI

To analyze network performance and determine the transmission slots for links to maximize network capacity and VoI, an ILP-based modeling approach can be employed to depict the link scheduling. Since the first-hop links are responsible for forwarding packets, network capacity is defined as the the number of direct links and second-hop links, while VoI is the sum of the value of these links. First, the relevant variables and parameters in the model are defined.

- x_l^t is a binary variable that represents the state of link l in slot t. $x_l^t = 1$ means that link l is assigned to slot t. Otherwise, it is 0.
- γ is the weight used to balance the importance of network capacity and VoI.
- $\mathcal{V}(l)$ represents the value of link l, which is equal to the value of the source node and can be calculated according to Eq. (1).
- $\mathcal{L}_{\text{Dir}}, \mathcal{L}_{\text{Fir}}, \mathcal{L}_{\text{Sec}}$ represent the sets of direct links, first-hop links, and second-hop links, respectively. $\mathcal{M}$ represents

the set of two-hop link pairs ($\mathcal{L}_{\text{Sec}} \rightarrow \mathcal{L}_{\text{Fir}}$). $\mathcal{L}_{\text{Dir}}(i)$ and $\mathcal{L}_{\text{Sec}}(i)$ represent the sets of direct and second-hop links with sub-node i as the receiver, respectively.

The formulated model for maximizing network capacity and VoI under complex constraints can be expressed as

$$\max \sum_{l\in\mathcal{L}_{\text{Dir}}\cup\mathcal{L}_{\text{Sec}}} \sum_{t\in\mathcal{T}} x_l^t \cdot (1+\gamma\cdot\mathcal{V}(l)),$$

subject to:

$$\sum_{t\in\mathcal{T}} x_l^t \leq 1, \quad \forall l \in \mathcal{L}. \tag{2a}$$

$$x_{l_i}^t + x_{l_j}^t \leq 1, \quad \forall t\in\mathcal{T}, l_i\in\mathcal{L}, l_j\in\mathcal{L}\setminus\{l_i\}, (l_i,l_j)\in\mathcal{C}. \tag{2b}$$

$$x_{l_{\text{sec}}}^{t'} \leq \sum_{t=1}^{t'-1} x_{l_{\text{fir}}}^t, \quad \forall t'\in\mathcal{T}\setminus\{1\}, (l_{\text{fir}}, l_{\text{sec}})\in\mathcal{M}. \tag{2c}$$

$$x_{l_{\text{fir}}}^k = 0, \quad \forall l_{\text{fir}}\in\mathcal{L}_{\text{Fir}}. \tag{2d}$$

$$x_{l_{\text{sec}}}^1 = 0, \quad \forall l_{\text{sec}}\in\mathcal{L}_{\text{Sec}}. \tag{2e}$$

$$\sum_{t\in\mathcal{T}} x_{l_{\text{fir}}}^t = \sum_{t\in\mathcal{T}} x_{l_{\text{sec}}}^t, \quad \forall (l_{\text{fir}}, l_{\text{sec}})\in\mathcal{M}. \tag{2f}$$

$$\sum_{l\in\mathcal{L}_{\text{Dir}}(i)\cup\mathcal{L}_{\text{Sec}}(i)} \sum_{t\in\mathcal{T}} x_l^t \geq 1, \quad \forall i\in\mathcal{N}. \tag{2g}$$

$$x_l^t \in \{0,1\}, \quad \forall l\in\mathcal{L}, t\in\mathcal{T}. \tag{2h}$$

Constraint (2a) ensures that each link is assigned at most one slot. Constraint (2b) prevents mutually exclusive links from being assigned to the same slot using the conflict matrix $\mathcal{C}$. Constraints (2c), (2d), and (2e) introduce the order of first-hop and second-hop links. Constraint (2f) guarantees the completeness of two-hop communication. Constraint (2g) is a task constraint that ensures all sub-nodes can receive usable information from source nodes with the same targets, in order to fulfill the task.

B. Heuristic Two-Step Search Algorithm

In Section III-A, the optimal network performance for resource allocation is presented considering global optimization. However, the resource allocation problem, when modeled as GCP, has been proven to be NP-complete [19]. Exact solutions are difficult to achieve in polynomial time. Therefore, heuristic algorithms are designed for practical systems.

Greedy algorithm, as a classical heuristic approach, typically performs well in solving the GCP. Based on this, a heuristic two-step search algorithm (TSA) is designed. The first step modifies the greedy algorithm to meet the two-hop communication and task constraints in the ILP model. The second step applies VNS with SA to optimize the initial solution and escape local optima. The detailed design of the algorithm is as follows.

First, some variables need to be defined in advance.

- $\mathcal{U}$: Set of uncovered links which do not satisfy the constraint (2g).
- $\mathcal{A}$: Set of covered links which satisfy the constraint (2g).
- $\mathcal{S}$: Set of nodes that satisfy the constraint (2g).
- $Con(l)$: Incremental contribution of link l to the joint objective.
- $Los(l)$: Decremental contribution of link l to the joint objective.
- $Score(l)$: Comprehensive evaluation of link l. Used to sort $\mathcal{U}$ and $\mathcal{A}$ in descending order.
- β: Weight of Los when calculating $Score$.
- r_i: Receiver of the link belongs to $\mathcal{L}_{\text{Dir}}$.
- d_i: Destination of the link belongs to $\mathcal{L}_{\text{Fir}}$.

Algorithm 1: Modified Greedy Algorithm (MGA)

```
Step 1: Traverse 𝓛.
  𝓤 ← {l ∈ 𝓛_Dir ∪ 𝓛_Fir}.
  𝓐 ← ∅.
Step 2: Define the sorting function.
for each pair (l_i, l_j) ∈ 𝓒 do
    if l_i ∈ 𝓤 ∪ 𝓐 then
        Con(l_i) = 1 + γ · 𝓥(l_i).
        if l_j ∈ 𝓛_Dir then
            Los(l_i) += 1 + γ · 𝓥(l_j).
        else
            Los(l_i) += (1+γ·𝓥(l_j))/2.
        end
    end
end
for each link l_i ∈ 𝓤 ∪ 𝓐 do
    Score(l_i) = Con_norm(l_i) − β · Los_norm(l_i).
end
Step 3: Sort 𝓤.
for each link l_i ∈ 𝓤 do
    if l_i ∈ 𝓛_Dir then
        if r_i ∈ 𝓢 then
            𝓐 ← 𝓐 ∪ {l_i}.
        else
            Select a conflict-free slot t ∈ 𝓣, x_{l_i}^t = 1.
        end
    else
        if d_i ∈ 𝓢 then
            𝓐 ← 𝓐 ∪ {l_i}.
        else
            Select conflict-free slots t ∈ 𝓣 and t' > t,
              x_{l_i}^t = 1 and x_{𝓜(l_i)}^{t'} = 1.
        end
    end
end
  Sort and traverse 𝓐 in the same way, without
  checking task constraint.
Step 4: Calculate the joint objective of network
  capacity and VoI. Additionally, the sorted 𝓤 and
  𝓐 from Step 3 serve as the initial solution 𝓧 in
  Algorithm 2.
```

The modified greedy algorithm (MGA) aims to obtain

Algorithm 2: Variable Neighborhood Search and Simulated Annealing (VNS-SA)

Step 1: Parameter Initialization.
Set initial temperature T_0, final temperature T_f, cooling rate η, and maximum iterations $I_{\max}$.

Step 2: Neighborhood Solution Generation.
Select one defined neighborhood structure for current solution $\mathcal{X}$ to generate candidate solution $\mathcal{X}'$.
1) Swap: Randomly swap $l_i, l_j \in \mathcal{X}$.
2) Insert: Randomly move $l_k \in \mathcal{X}$ to a new place.
3) Reverse: Reverse $\{l_m, \ldots, l_n\} \subseteq \mathcal{X}$.

Step 3: Solution Evaluation.
Calculate the joint objective difference
$\Delta f = f(\mathcal{X}') - f(\mathcal{X})$.
if $\Delta f > 0$ **then**
| Accept $\mathcal{X}'$.
else
| Accept with probability $P = \exp(\Delta f / T)$.
end

Step 4: Dynamic Cooling and Termination.
Update temperature $T \leftarrow \eta T$.
if $T < T_f$ *or* I_{max} *are reached* **then**
| Output the optimal solution $\mathcal{X}_{\text{best}}$.
else
| Return to **Step 2**.
end

a feasible initial solution, reducing the difficulty of global search. By simultaneously allocating two available slots for first-hop and second-hop links to satisfy two-hop communication constraints. Subsequently, sets $\mathcal{U}$ and $\mathcal{A}$ satisfy the task constraint, and the link sorting function is adapted based on VoI, as detailed in **Algorithm 1**.

Based on the greedy initial solution, the VNS enhances search diversity by sequentially executing predefined neighborhood structures, which involve modifying the link sorting in sets $\mathcal{U}$ and $\mathcal{A}$. These neighborhood structures may include link swapping, reversing the order of a region, or inserting links into random positions. When combined with SA, the algorithm accepts worse solutions during the search with a dynamic probability, helping to avoid local optima. As the temperature decreases, the probability of accepting worse solutions gradually reduces and the algorithm ultimately stabilizes. Detailed steps are provided in **Algorithm 2**.

IV. Simulation Validation and Performance Analysis

In this section, the simulation results are presented to demonstrate the effectiveness of the proposed algorithm. NS-3 is used to model the random movement of the jammer and implement the proposed TSA on the central node. The simulation environment is configured as Table I. Moreover, the normal distribution model in NS-3 is utilized to generate VoP for each node. The arithmetic mean is a nonlinear monotonically increasing function of distance, while the variance is selected from a random interval. The simulation assumes the communication rate of each link as R [16]. Network capacity is defined as the throughput within one resource allocation cycle, measured in units of R. Similarly, network VoI is defined as the sum of VoL within the same resource allocation cycle and is dimensionless.

TABLE I
Configuration of simulation environment

Parameters	Values
Number of sub-nodes: n	30
Number of jammers	1
Number of task targets: p	5
Network coverage	30 km $\times$ 30 km
Directional communication range	20 km
Beamwidth	45°
Control period duration	80 ms
Communication period duration	1000 ms
Slot duration	1 ms
Resource allocation cycle: $\mathcal{T}$	5 (length), 200 (number)
Tuning parameter: α	2.0
$\mathcal{V}_{max}$	100
$\mathcal{V}_{min}$	0
Weight of VoI: γ	1
Weight of Los: β	0.1
Initial temperature: T_0	1000
Final temperature: T_f	0.1
Cooling rate: η	0.995
Maximum iterations: $I_{\max}$	2000

The mathematical model established in Section III-A is first solved by Gurobi [20] to obtain the theoretical upper bounds of network capacity and VoI, and then a detailed analysis of the performance of TSA is conducted.

Fig. 3(a) and 3(b) illustrate the evolution of network capacity and VoI over time in the presence of dynamic interference, respectively. Due to the random walk model applied to sub-nodes and the movement of the jammer along random paths, the continuous variation in VoP leads to fluctuations in the observed performance. The simulation results show that MGA achieves, on average, 85% of the theoretical optimal value. Subsequently, TSA enhances the performance to 94% on average. This improvement is attributed to the centralized structure of the network, which enables the central node to conduct a global search and find a near-optimal solution during the decision-making phase.

In Fig. 4, the number of sub-nodes is shown to vary from 10 to 50 to further verify the performance of TSA. It is shown in Fig. 4(a) and 4(b) that as the number of sub-nodes increases, the performance of MGA witnesses a successive decrease. However, TSA can still obtain near-optimal solutions. This is due to MGA's tendency to fall into local optima. In contrast, TSA overcomes this limitation by dynamically adjusting the neighborhood structure, which can maintain better performance.

V. Conclusion

In this paper, a heuristic two-step search algorithm was proposed as a near-optimal solution for spatio-temporal resource

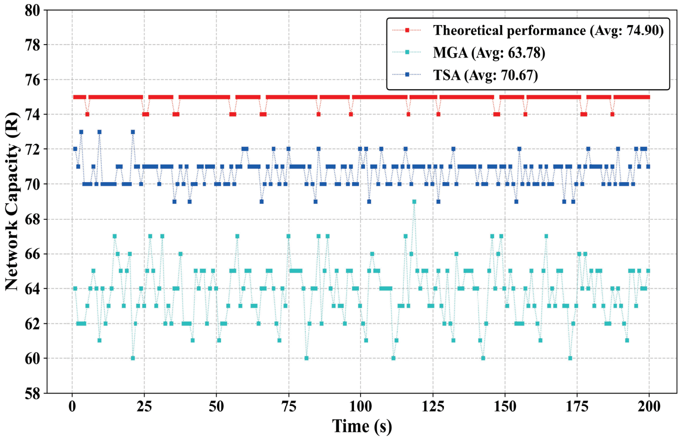

(a) The variation of network capacity versus time.

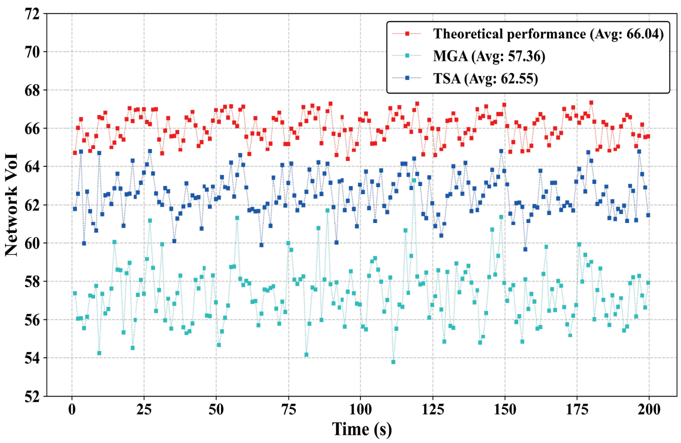

(b) The variation of network VoI versus time.

Fig. 3: Real-time Network capacity and VoI under dynamic interference.

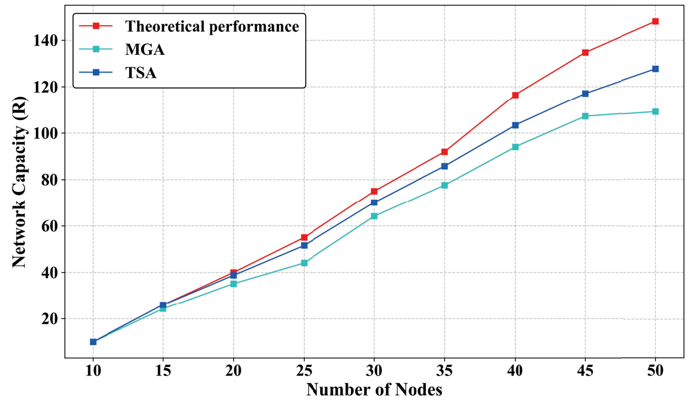

(a) The variation of network capacity versus nodes.

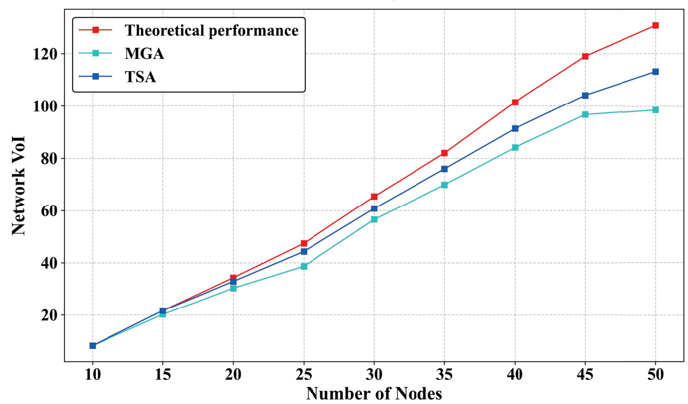

(b) The variation of network VoI versus nodes.

Fig. 4: Results of Network capacity and VoI across different nodes.

allocation in task-oriented single-beam directional WNs. To delineate the theoretical bounds of network capacity and VoI, an ILP-based modeling approach was proposed. Furthermore, to balance computational complexity and optimization performance, a greedy algorithm was adapted to obtain an initial solution satisfying task-specific constraints, followed by a utilization of variable neighborhood search and simulated annealing to enhance the solution quality. Simulation results show that the TSA can achieve near-optimal network capacity and VoI under dynamic interference, and its effectiveness can be maintained across different numbers of nodes.

References

[1] M. T. Mahmud et al., "Cooperation-based adaptive and reliable MAC design for multichannel directional wireless IoT networks," *IEEE Access*, vol. 9, pp. 97518–97538, 2021.

[2] M. S. Bahbahani et al., "A directional TDMA protocol for high throughput URLLC in mmWave vehicular networks," *IEEE Trans. Veh. Technol.*, vol. 72, no. 3, pp. 3584–3599, Mar. 2023.

[3] O. Ayan et al., "Semantics- and task-oriented scheduling for networked control systems in practice," *IEEE Access*, vol. 10, pp. 115673–115690, 2022.

[4] J. Liu et al., "Task-oriented intelligent networking architecture for the space–air–ground–aqua integrated network," *IEEE Internet Things J.*, vol. 7, no. 6, pp. 5345–5358, Jun. 2020.

[5] W. Wang et al., "Value matters: A novel value of information-based resource scheduling method for CAVs," *IEEE Trans. Veh. Technol.*, vol. 73, no. 6, pp. 8720–8735, Jun. 2024.

[6] J. Jiang et al., "A medium access control protocol based on parity group-graph coloring for underwater AUV-aided data collection," *IEEE Internet Things J.*, vol. 11, no. 4, pp. 5967–5979, Feb. 2024.

[7] D. Yu et al., "Implementing the abstract MAC layer via inductive coloring under the Rayleigh-fading model," *IEEE Trans. Wireless Commun.*, vol. 20, no. 9, pp. 6167–6178, Sept. 2021.

[8] S. Garg et al., "A real-time, distributed, directional TDMA MAC protocol for QoS-aware communication in multi-hop wireless networks," *IEEE Access*, vol. 9, pp. 26343–26361, 2021.

[9] F. A. Alfouzan et al., "A collision-free graph coloring MAC protocol for underwater sensor networks," *IEEE Access*, vol. 7, pp. 39862–39878, 2019.

[10] S. Guo et al., "Joint resource allocation and power control for full-duplex V2I communication in high-density vehicular network," *IEEE Trans. Wireless Commun.*, vol. 21, no. 11, pp. 9497–9508, Nov. 2022.

[11] S. van den Elzen et al., "Dynamic network visualization with extended massive sequence views," *IEEE Trans. Vis. Comput. Graphics*, vol. 20, no. 8, pp. 1087–1099, Aug. 2014.

[12] M. Gutierrez et al., "A reduced variable neighbourhood search for the beam angle optimisation problem," *IEEE Trans. Emerg. Topics Comput. Intell.*, vol. 7, no. 5, pp. 1499–1510, Oct. 2023.

[13] X. Wu et al., "Multiregion mission planning by satellite swarm using simulated annealing and neighborhood search," *IEEE Trans. Aerosp. Electron. Syst.*, vol. 60, no. 2, pp. 1416–1439, Apr. 2024.

[14] Y. Shen et al., "ECMAC: Edge-assisted cluster-based MAC protocol in software-defined vehicular networks," *IEEE Trans. Veh. Technol.*, vol. 73, no. 9, pp. 13738–13750, Sept. 2024.

[15] P. Gjanci et al., "Path Finding for Maximum Value of Information in Multi-Modal Underwater Wireless Sensor Networks," *IEEE Trans.*

Mobile Comput., vol. 17, no. 2, pp. 404–418, Feb. 2018.

[16] J. Zhang et al., "Distributed time resource allocation algorithm for multi-beam directional ad-hoc networks," *IEEE Commun. Lett.*, vol. 28, no. 6, pp. 1357–1361, Jun. 2024.

[17] M. Adil et al., "Enhanced-AODV: A robust three phase priority-based traffic load balancing scheme for Internet of Things," *IEEE Internet Things J.*, vol. 9, no. 16, pp. 14426–14437, Aug. 2022.

[18] Z. Chu et al., "Exclusive-region-map-based medium access control in mobile networks with directional antennas through deep interference learning," *IEEE Trans. Cogn. Commun. Netw.*, vol. 9, no. 4, pp. 1012–1024, Aug. 2023.

[19] I. Holyer, "The NP-completeness of edge-coloring," *SIAM J. Comput.*, vol. 10, no. 4, pp. 718–720, 1981.

[20] Gurobi Optimization, LLC, "Gurobi Optimizer Reference Manual," 2024. [Online]. Available: https://www.gurobi.com